

## Pressure-Induced Non-Fermi-Liquid Behavior of PrNiO<sub>3</sub>

J.-S. Zhou,<sup>1</sup> J. B. Goodenough,<sup>1</sup> and B. Dabrowski<sup>2</sup>

<sup>1</sup>Texas Materials Institute, ETC 9.102, University of Texas at Austin, 1 University Station, C2201, Austin, Texas 78712, USA

<sup>2</sup>Department of Physics, Northern Illinois University, DeKalb, Illinois 60115, USA

(Received 22 January 2004; revised manuscript received 30 August 2004; published 9 June 2005)

Comprehensive temperature scans of the resistivity of a high-quality sample of PrNiO<sub>3</sub> were made under different pressures up to 30 kbar; they have revealed that the insulator phase is suppressed completely at  $P \approx 13$  kbar, transforming to a non-Fermi-liquid phase in which the resistivity varies as  $\Delta\rho = \rho(T) - \rho_0 \sim T^n$  with  $n = 1.33$  and  $1.60$  over a broad pressure range.

DOI: 10.1103/PhysRevLett.94.226602

PACS numbers: 72.80.-r, 71.27.+a, 71.28.+d, 71.30.+h

The  $\sigma$ -bonding electrons of the RNiO<sub>3</sub> perovskites undergo evolution from an enhanced Pauli paramagnetism in metallic LaNiO<sub>3</sub> to an antiferromagnetic insulator with Curie-Weiss paramagnetism in SmNiO<sub>3</sub> as the ionic radius of the  $R^{3+}$  ion decreases [1,2]. As the  $R^{3+}$ -ion radius increases from Lu to Sm, the Néel temperature  $T_N$  increases and a first-order insulator-metal (IM) transition temperature  $T_{IM}$  decreases until  $T_N = T_{IM}$  in NdNiO<sub>3</sub> and PrNiO<sub>3</sub>. There is no anomaly in the temperature dependence of the paramagnetic susceptibility on crossing  $T_{IM} > T_N$  [2]; the Ni-O bond length on the insulator side of  $T_{IM}$  is intermediate between the metallic and the ionic equilibrium Ni-O bond lengths [3]. These characteristics of the IM transition are in sharp contrast to those found at the Mott transition in V<sub>2</sub>O<sub>3</sub>, for example [4]. In the phase diagram of the RNiO<sub>3</sub> family,  $T_{IM}$  falls to zero at the composition  $x \approx 0.5$  of La<sub>1-x</sub>Pr<sub>x</sub>NiO<sub>3</sub> [5]. Physical properties associated with an order-disorder transition, even if it is first order, may develop some quantum critical characteristics as the transition temperature is reduced to near zero by a variation of parameters such as chemical composition, pressure, or an applied magnetic field [6]. New ground states commonly develop on the disorder side of the transition in the vicinity of a quantum critical point (QCP). Critical spin fluctuations at the QCP of a magnetic transition can result in non-Fermi-liquid (NFL) behavior [7–9] or even mediate superconductive pairing [10]. Previous measurements of  $\rho(T)$  on PrNiO<sub>3</sub> [11–13] show that the IM transition and hysteresis loop vanish at  $P_c \approx 13$  kbar. However, poor data quality due to porous samples prevents an adequate characterization of the metallic phase at  $P > 13$  kbar. The high-quality sample used in this work and an enhanced capacity of our piston-cylinder device allowed us to explore much more accurately the metallic phase in the vicinity of  $P_c$  and, more importantly, how the metallic phase evolves as pressure increases far beyond  $P_c$ . We have also made a comparison between the metallic phase of PrNiO<sub>3</sub> at highest pressure with LaNiO<sub>3</sub>. Almost all NFL phases reported are formed in the vicinity of critical parameters ( $P_c$ ,  $x_c$ , and  $H_c$ ) where a magnetic transition in a Fermi-liquid (FL) metallic phase is suppressed. We investigate whether the transition from the antiferromagnetic

insulator to the metallic phase in PrNiO<sub>3</sub> ends, under pressure, in a NFL phase and whether the NFL phase is the same or different from those previously reported for other NFL systems.

High-quality RNiO<sub>3</sub> samples have been fabricated by the cold-press technique described in a previous paper [14]. Cu wires were pressed onto the sample on small pieces of In foil. The contact resistance is less than 1  $\Omega$ . The high-pressure experiments were performed with a self-clamped Cu-Be cell to 3 GPa [13]. For comparison with results obtained by others on porous samples, we highlight a few remarkable aspects of the  $\rho(T)$  curves of Fig. 1 on these high-quality samples: (1) The magnitude of  $\rho(300$  K) of the RNiO<sub>3</sub> samples  $R = \text{La, Pr, Nd}$  decreases with increasing Ni-O-Ni bond angle  $\theta$  [3]. (2) The  $\rho(300$  K) is significantly lower than has been reported in the literature, including that of a single-crystal NdNiO<sub>3</sub> film [15] shown in Fig. 1. (3) The residual resistivity  $\rho_0 \approx 6$   $\mu\Omega$  cm of the curves is smaller by at least a factor of 4 than the lowest  $\rho_0$  previously reported for LaNiO<sub>3</sub> or PrNiO<sub>3</sub> under  $P > 14$  kbar; moreover, a pressure-independent  $\rho_0$  shows there is no grain-boundary effect

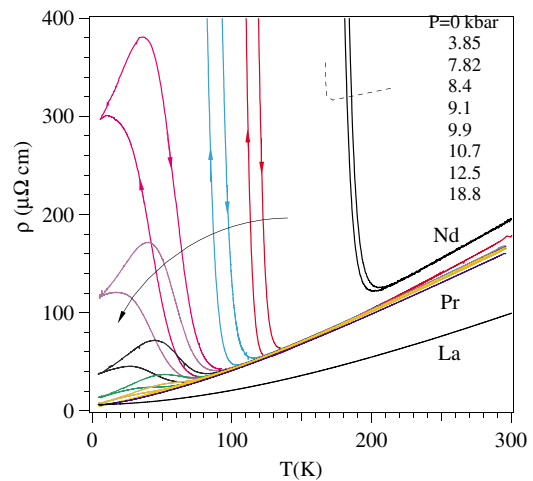


FIG. 1 (color online). Temperature dependence of the resistivity  $\rho$  for RNiO<sub>3</sub> and PrNiO<sub>3</sub> under pressure. The dashed line represents  $\rho(T)$  for a NdNiO<sub>3</sub> film from Ref. [16].

in these high-quality samples. (4) High ratios  $\rho(300\text{ K})/\rho_0 = 17$  for  $\text{LaNiO}_3$  and 27 for  $\text{PrNiO}_3$  under  $P > P_c$  compares with reported ratios 4 to 9.5 for  $\text{LaNiO}_3$  and 20 for  $\text{PrNiO}_3$  under pressure, respectively. The analysis of the  $\rho(T)$  leads us to the conclusion that a NFL phase is achieved in  $\text{PrNiO}_3$  as the insulator phase is suppressed under pressure.

Figure 1 includes a succession of  $\rho(T)$  curves for  $\text{PrNiO}_3$  under increasing pressure;  $T_{\text{IM}} \approx 130\text{ K}$  at ambient pressure moves progressively to lower temperature under pressure and the thermal hysteresis loop broadens. Unlike  $\text{BaVS}_3$  [16] where the IM transition remains sharp as  $T_c$  is lowered under pressure, the IM transition in  $\text{PrNiO}_3$  becomes much broader and more difficult to define as  $T_{\text{IM}}$  falls below 70 K. The hysteresis loop persists to around 50–60 K, but at pressures  $P > 10.7\text{ kbar}$  there is no low-temperature upturn of the resistivity to mark  $T_{\text{IM}}$ . With the best resolution in our measurement, a homogeneous metallic phase without a hysteresis loop is achieved under  $P \geq 13\text{ kbar}$ . In order to analyze the metallic phase stabilized under pressure, we have applied the power-law fitting to  $\rho(T)$  of  $\text{PrNiO}_3$  under pressure along with that of metallic  $\text{LaNiO}_3$ . Whereas a Fermi-liquid phase, namely,  $\Delta\rho(T) = \rho(T) - \rho_0 \sim T^n$  with  $n = 2$ , is observed in  $\text{LaNiO}_3$  under ambient pressure, an  $n < 2$  has been ob-

tained for the metallic phase of  $\text{PrNiO}_3$  under pressure. As demonstrated in Fig. 2, the power-law formula with  $n = 4/3$  fits the experimental data extremely well for the pressure range 8–20 kbar. The exponent  $n$  jumps to about 1.60 for the pressure range 20–30 kbar. The pressure dependence of the exponent  $n$  is plotted in Fig. 3 together with the evolution with pressure of the transition temperature  $T_{\text{IM}}$ . Curve fitting in the metallic phase is made within  $5 \leq T \leq 20\text{ K}$ , but the fitting curve based on this temperature range remains matched to  $\rho(T)$  up to  $T_u = 100\text{ K}$  for pressures around 20 kbar;  $T_u$  falls gradually to about 50–60 K on further increase of pressure. Significantly, this low-temperature metallic phase does not show a clear trend to a FL phase under the highest pressure of this work. Moreover, the extension to higher pressure of a formula fitting to the resistivity at 285 K versus  $P$  (inset of Fig. 3) appears not to meet the  $\rho(285\text{ K})$  of  $\text{LaNiO}_3$  at any pressures below 60 kbar, whereas a recent structural study [17] under high pressure places the orthorhombic-rhombohedral transition in  $\text{PrNiO}_3$  at  $P_c \approx 50\text{ kbar}$ . These observations point out that the transition at low temperature from the orthorhombic NFL phase to the rhombohedral FL phase is going to be first order, which means that a FL phase may be realized only in the rhombohedral phase having a broader bandwidth than the orthorhombic phase. However, it is not yet clear at this point whether a first-order transition is required for the electronic state change on crossing the phase boundary between the NFL phase and a FL phase since the orthorhombic to rhombohedral structural transition is always first order in perovskite oxides [18].

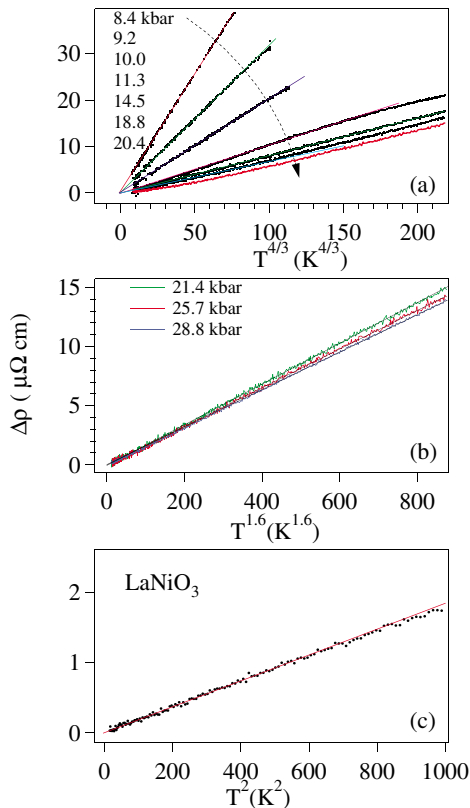


FIG. 2 (color online). (a)  $\rho$  versus  $T^{4/3}$  for  $\text{PrNiO}_3$  for  $8 < P < 20\text{ kbar}$ ; (b)  $\rho(T)$  versus  $T^{1.6}$  for  $P > 20\text{ kbar}$ ; (c)  $\rho$  versus  $T^2$  for  $\text{LaNiO}_3$  under ambient pressure.

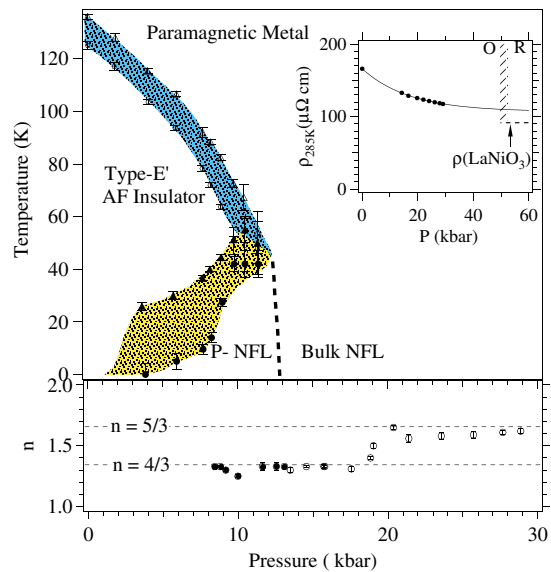


FIG. 3 (color online). The pressure-temperature phase diagram of  $\text{PrNiO}_3$  and pressure dependence of the exponent  $n$  in  $\Delta\rho \sim T^n$ . The shadowed area represents the thermal hysteresis in  $\rho(T)$ . P-NFL stands for the percolated non-Fermi-liquid phase.

As shown in Figs. 1 and 2, the reentrant metallic phase on warming up from 5 K under  $8 < P < 10$  kbar can also be fit to a power law with  $n \approx 4/3$ , marked as solid circles in Fig. 3. It could be argued that the NFL behavior is related to phase inhomogeneity since a huge hysteresis loop is found in  $\rho(T)$  under these pressures. However, we emphasize here that the NFL phase is stabilized over a broad range of pressure  $13 \leq P < 30$  kbar where no thermal hysteresis of  $\rho(T)$  has been observed. Therefore, the NFL behavior has nothing to do with a phase inhomogeneity. Instead, the transport property in the mixed-phase region should be dominated by the more conductive phase, i.e., a percolated connection of the NFL phase. In Fig. 3, the region of a percolated NFL phase is separated by a dashed line near 13 kbar from the bulk NFL at higher pressures.

A  $\rho(T)$  following a power law with  $n < 2$  at low temperatures has been generally argued to be caused by quantum critical fluctuations, and this behavior has been found in a metal where a spin ordering is suppressed under magnetic field or pressure [7–10]. Millis *et al.* [19] have predicted that quantum critical fluctuations lead to a power law with  $n = 4/3$  in a two-dimensional system near the end point of a first-order transition. This prediction fits very well to the lower step  $n \approx 4/3$  in Fig. 3 even though PrNiO<sub>3</sub> has a 3D perovskite structure. On the other hand, the pressure-temperature phase diagram of Fig. 3 is surprisingly similar to that of a Mott insulator  $\kappa - (\text{BEDT} - \text{TTF})_2\text{Cu}[\text{N}(\text{CN})_2]\text{Cl}$  under pressure [20]. In this case quantum critical fluctuations near the end point of a Mott transition gives rise to superconductive pairing. On the left-hand side of the critical point in that phase diagram, a percolated superconducting phase has been detected within the insulator phase whereas a percolated NFL phase has been identified below 13 kbar in PrNiO<sub>3</sub>. Moreover, it is clear from Fig. 3 that the NFL phase found in PrNiO<sub>3</sub> is not confined to the vicinity of  $P_c$ , but extends to much higher pressures as has been reported for MnSi [21,22] in which the ferromagnetic transition is suppressed at  $P_c = 14$  kbar and the NFL remains stable under pressure up to 30 kbar. However, two distinct exponents  $n$  that are close to the fractional numbers  $4/3$  and  $5/3$  distinguish the NFL phase of PrNiO<sub>3</sub> from that in MnSi. This interesting feature calls for an experiment at even higher pressure ( $\sim 50$  kbar) in order to check whether  $n$  approaches  $n = 2$  by steps of a fractional number.

As to the nature of the IM transition in PrNiO<sub>3</sub>, which can be important for understanding the NFL behavior in which it terminates, we have made precise temperature scans of  $\rho(T)$  and the thermal conductivity  $\kappa(T)$  around the transition and compared them with some well-known transitions in manganites and magnetite. As shown in Fig. 1, the reentrant metallic phase, which is more clearly shown on the warming up loop, develops at a  $T < T_{\text{IM}}$  with increasing pressure. The merging of two first-order transitions leaves a giant thermal hysteresis loop of  $\rho(T)$  and

an unusual circling of  $\rho(T)$  for the reentrant metallic phase in comparison with that for the metal-insulator transition at  $T_c$  in  $(\text{La}_{0.25}\text{Nd}_{0.75})_{0.7}\text{Ca}_{0.3}\text{MnO}_3$  under 7.5 kbar [23]. Typical  $\rho(T)$  curves taken in the pressure range 8–10 kbar are shown in Fig. 4. On warming up from 5 K,  $\rho(T)$  is precisely reproducible to that on cooling down—see Fig. 4(c)—as long as the upper bound temperature is below a  $T_{\text{max}}$  where resistivity shows a maximum on warming. It is within this temperature range that we carried out a curve fitting to the power law.

As a widely used explanation of the IM transition in RNiO<sub>3</sub> [24], charge disproportionation or bond-type ordering can be expected to enhance the thermal conductivity  $\kappa(T)$  as found at the Verwey transition of Fe<sub>3</sub>O<sub>4</sub> in Fig. 5(b) and orbital or charge ordering in La<sub>1.875</sub>Sr<sub>0.125</sub>MnO<sub>3</sub> [25]. In contrast to an enhancement below a critical temperature, the thermal conductivity of PrNiO<sub>3</sub> shown in Fig. 5(a), collapses below  $T_{\text{IM}}$  even after taking into account the change in the electronic contribution. This observation suggests that even the lattice undergoes critical fluctuations in the insulator phase below a  $T_{\text{Im}} \leq 130$  K. Alternatively, as indicated in Fig. 3, a collapse of  $\kappa$  in the insulator phase below  $T_{\text{IM}}$  can be attributed to a two-phase mixture of the magnetic-insulator phase and the NFL phase at ambient pressure. In either case, lattice (charge) and spin should exhibit critical fluctuations near the end point of  $T_{\text{IM}}$ . These

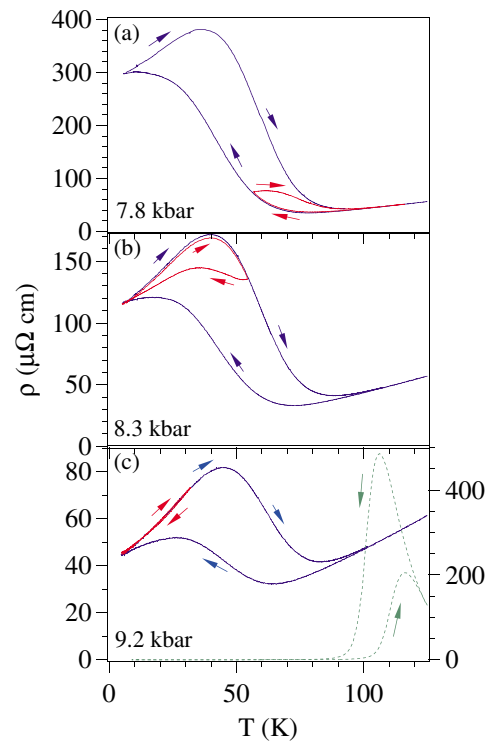


FIG. 4 (color online).  $\rho(T)$  of PrNiO<sub>3</sub> under different pressures for various temperature-scan loops. Plotted in (c) as a dashed line is the  $\rho(T)$  in  $(\text{La}_{0.25}\text{Nd}_{0.75})_{0.7}\text{Ca}_{0.3}\text{MnO}_3$  under  $p = 7.5$  kbar for comparison.

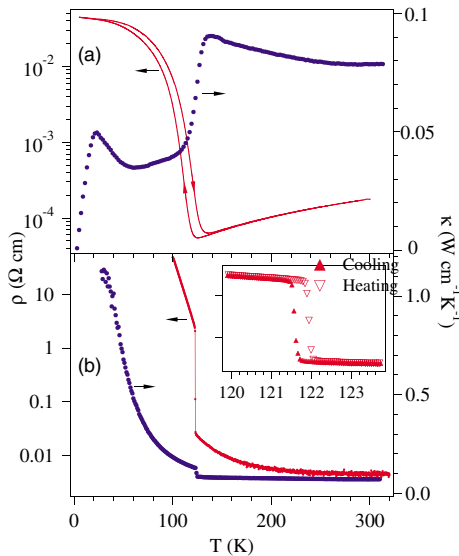


FIG. 5 (color online). Temperature dependence of the resistivity  $\rho$  and thermal conductivity  $\kappa$  for (a)  $\text{PrNiO}_3$  at ambient pressure, and (b) an  $\text{Fe}_3\text{O}_4$  crystal.

fluctuations are likely to have quantum effects below a Fermi degeneracy temperature as proposed by Imada [26]. Spin and charge fluctuations near an end point of  $T_{\text{IM}}$  distinguish the NFL phase in  $\text{PrNiO}_3$  from that found at end points of a magnetic transition in a metal and a Mott transition. On the other hand, separated only by a tiny margin of bandwidth [3],  $\text{LaNiO}_3$  shows a well-classified Fermi-liquid behavior up to 28 K. The coefficient  $A = 1.8 \times 10^{-3} \mu\Omega \text{ cm K}^{-2}$  of  $\rho(T) = \rho_0 + AT^2$  for  $\text{LaNiO}_3$  is comparable to that found in other strongly correlated metallic oxides such as  $\text{La}_{1.7}\text{Sr}_{0.3}\text{CuO}_4$  and  $\text{Sr}_2\text{RuO}_4$  [27].

In conclusion, the metallic phase in  $\text{PrNiO}_3$  at  $P > 13$  kbar where the metal-insulator transition temperature is terminated, has been found not to follow the description of Fermi-liquid theory. A power-law fitting to  $\rho(T)$  of this metallic phase gives two distinct exponents, an  $n \approx 1.33$  over the pressure range 8–20 kbar and an  $n \approx 1.60$  in the range 20–30 kbar. Although a percolated NFL metallic phase may exist in the pressure range  $8 < P < 13$  kbar, a bulk NFL phase exists at higher pressures, and the step in the exponent  $n$  at 20 kbar remains as a novel feature needing theoretical attention. This non-Fermi-liquid phase appears to be caused by both lattice (charge) and spin fluctuations where the transition temperature  $T_{\text{IM}} = T_{\text{N}}$  is terminated under pressure. The results also suggest that a Fermi-liquid metallic phase can be achieved in the perovskites  $R\text{NiO}_3$  family only with rhombohedral symmetry.

The authors thank the NSF for Grants No. DMR 0132282 (J.B.G.) and No. DMR 0302617 (B.D.) and the Robert A. Welch Foundation of Houston, Texas, for financial support.

- [1] J. B. Torrance, P. Lacorre, A. I. Nazzal, E. J. Ansaldo, and Ch. Nidermayer, *Phys. Rev. B* **45**, 8209 (1992).
- [2] J.-S. Zhou, J. B. Goodenough, B. Dabrowski, P. W. Klamut, and Z. Bukowski, *Phys. Rev. Lett.* **84**, 526 (2000).
- [3] J.-S. Zhou and J. B. Goodenough, *Phys. Rev. B* **69**, 153105 (2004).
- [4] D. B. McWhan, A. Menth, J. P. Remeika, W. F. Brinkman, and T. M. Rice, *Phys. Rev. B* **7**, 1920 (1973).
- [5] M. Medarde, *J. Phys. Condens. Matter* **9**, 1679 (1997).
- [6] S. Sachdev, *Quantum Phase Transitions* (Cambridge University Press, Cambridge, 1999).
- [7] N. Doiron-Leyraud, I. R. Walker, L. Taillefer, M. J. Steiner, S. R. Julian, and G. G. Lonzarich, *Nature (London)* **425**, 595 (2003).
- [8] J. Custers, P. Gegenwart, H. Wilhelm, K. Neumaler, Y. Toklwa, O. Trovarelli, G. Geibel, F. Steglich, C. Pepin, and P. Coleman, *Nature (London)* **424**, 524 (2003).
- [9] K. H. Kim, N. Harrison, M. Jaime, G. S. Boebinger, and J. A. Mydosh, *Phys. Rev. Lett.* **91**, 256401 (2003).
- [10] N. D. Mathur, F. M. Grosche, S. R. Julian, I. R. Walker, D. M. Freye, R. K. W. Haselwimmer, and G. G. Lonzarich, *Nature (London)* **394**, 39 (1998).
- [11] X. Obradors, L. M. Paulius, M. B. Maple, J. B. Torrance, A. I. Nazzal, J. Fontcuberta, and X. Granados, *Phys. Rev. B* **47**, 12353 (1993).
- [12] P. C. Canfield, J. D. Thompson, S.-W. Cheong, and L. W. Rupp, *Phys. Rev. B* **47**, 12357 (1993).
- [13] J.-S. Zhou, J. B. Goodenough, B. Dabrowski, P. W. Klamut, and Z. Bukowski, *Phys. Rev. B* **61**, 4401 (2000).
- [14] J.-S. Zhou, J. B. Goodenough, and B. Dabrowski, *Phys. Rev. B* **67**, 020404 (2003).
- [15] U. Staub, G. I. Meijer, F. Fauth, R. Allenspach, J. G. Bednorz, J. Karpinski, S. M. Kazakov, L. Paolasini, and F. d'Acapito, *Phys. Rev. Lett.* **88**, 126402 (2002).
- [16] L. Forro, R. Gaal, H. Berger, P. Fazekas, K. Penc, I. Kezsmarki, and G. Mihaly, *Phys. Rev. Lett.* **85**, 1938 (2000).
- [17] J.-S. Zhou, J. B. Goodenough, and B. Dabrowski, *Phys. Rev. B* **70**, 081102 (2004).
- [18] J.-S. Zhou and J. B. Goodenough, *Phys. Rev. Lett.* **94**, 065501 (2005).
- [19] A. J. Millis, A. J. Schofield, G. G. Lonzarich, and S. A. Grigera, *Phys. Rev. Lett.* **88**, 217204 (2002).
- [20] F. Kagawa, T. Itou, K. Miyagawa, and K. Kanoda, *Phys. Rev. B* **69**, 064511 (2004).
- [21] C. Pfleiderer, D. Reznik, L. Pintschovius, H. v. Lohneysen, M. Garst, and A. Rosch, *Nature (London)* **427**, 227 (2004).
- [22] C. Pfleiderer, S. R. Julian, and G. G. Lonzarich, *Nature (London)* **414**, 427 (2001).
- [23] J.-S. Zhou, W. Archibald, and J. B. Goodenough, *Nature (London)* **381**, 770 (1996).
- [24] J. A. Alonso, J. L. Garcia-Munoz, M. T. Fernandez-Diaz, M. A. G. Aranda, M. J. Martinez-Lope, and M. T. Casais, *Phys. Rev. Lett.* **82**, 3871 (1999).
- [25] J.-S. Zhou and J. B. Goodenough, *Phys. Rev. B* **64**, 024421 (2001).
- [26] M. Imada, *J. Phys. Soc. Jpn.* **73**, 1851 (2004).
- [27] S. Nakamae, K. Behnia, N. Mangkorntong, M. Nohara, H. Takagi, S. J. C. Yates, and N. E. Hussey, *Phys. Rev. B* **68**, 100502(R) (2003).